Electronic Supplementary Material (ESI) for Chemical Communications.
This journal is © The Royal Society of Chemistry 2015

Supplementary Information

Efficient light-driven water oxidation catalyzed by a mononuclear cobalt (III) complex

Yukun Zhao,[a] Junqi Lin,[a] Yongdong Liu,[a] Baochun Ma[a], Yong Ding*[ab] and Mindong Chen[b]

[a]State Key Laboratory of Applied Organic Chemistry, Key Laboratory of Nonferrous Metal Chemistry and Resources Utilization of Gansu Province and College of Chemistry and Chemical Engineering, Lanzhou University, Lanzhou 730000, China.

[b]Jiangsu Key Laboratory of Atmospheric Environment Monitoring and Pollution Control (AEMPC)，School of Environmental Sciences and Engineering, Nanjing University of Information Science and Technology, Nanjing 210044, China.

* To whom correspondence should be addressed.
E-mail: dingyong1@lzu.edu.cn

Experimental Section

Materials

All chemicals used for synthesizing catalysts were obtained from a chemical company and used without further purification. Purified water (18.2 MΩ·cm) for the preparation of solutions was obtained from a Molecular Lab Water Purifier.

Synthesis of complex 1

$CoCl_2·6H_2O$ (0.5 mmol, 119.1 mg) was dissolved in 4 mL of acetonitrile and a purple solution (1) was obtained. Na_2CO_3 (0.5 mmol, 53.0 mg) and di(2-pyridyl)ketone (1.0 mmol, 184.0 mg) (1:2) were dissolved into a mixed solution (2) of distilled water and acetonitrile (V_{water}:$V_{acetonitrile}$=1:1, 8mL) and the mixture was stirring until a clear solution was formed. Then, solution 1 was slowly dropwise added to solution 2 with strong stirring and the colour of mixture solution was gradually becoming dark-red in the air. The solution was strongly stirred for 2-3 hours, and then filtered. The filtrate was kept in a 20 mL flasket to allow slow evaporation at room temperature and the dark-red crystals (yield based on cobalt: 17 %) were obtained after 3-5 days. The product was further purified by silica gel column chromatography (CH_2Cl_2/CH_3OH = 1:2). ∠O1,Co1,O1a 179.999(1)^{o}; ∠O1,Co1,N1 83.0(2)^{o}; ∠O1,Co1,N1a 97.0(2) ^{o}; ∠N1,Co1,N1a 179.999(2)^{o}; ∠N1,Co1,N2 89.6(3)^{o}; ∠N1,Co1,N2a 90.4(3)^{o}; ∠N2,Co1,N2a 179.999(1)^{o}. IR (KBr): 3259, 3073, 2311, 1697, 1669, 1603, 1567, 1462, 1442, 1287, 1195, 1157, 1092, 1026, 1007,937, 906, 816, 791, 770, 735, 672, 600, 556, 486, 464, 406 cm^{-1}. ^{1}HNMR: 2.56ppm (s, 2H); 7.95ppm (d, 4H); 8.12ppm (m, 4H); 7.38ppm (m, 4H); 8.30ppm (d, 4H). UV-vis: 380 nm, 470 nm, 550 nm.

Synthesis of complex 2

$CuCl_2·2H_2O$ (0.5 mmol, 85.3 mg) was dissolved in 4 mL of acetonitrile and a purple solution (3) was obtained. Di(2-pyridyl)ketone (1.0 mmol, 184.0 mg) was dissolved into a mixed solution (4) of distilled water and acetonitrile (V_{water}:$V_{acetonitrile}$ =1:1, 8mL) and the mixture was stirring until a clear solution was formed. Then, solution 3 was dropwise added to solution 4 with strong stirring and the colour of mixture solution was gradually becoming dark-blue in the air. The solution was strong stirred for 1-2 hours, and then filtered. The filtrate was kept in a 20 mL flasket to allow slow evaporation at room temperature and the dark-blue crystals (yield based on copper: 11 %) was obtained after 3-5 days. The product was further purified by silica gel column chromatography (CH_2Cl_2/CH_3OH = 1:2). IR (KBr): 3432, 3348, 3204, 2818, 2321, 2234, 2113, 2030, 1996, 1951, 1889, 1826, 1607, 1571, 1467, 1444, 1419, 1300, 1290, 1268, 1217,1167, 1091, 1053, 1031, 1016, 931,906, 804, 784, 765, 672, 650, 617, 574, 433 cm^{-1}.

Synthesis of complex 3-5

Complex **3-5** was synthesized according to previous literatures.[1-3]

Catalysts characterization

Cyclic voltammetry (CV) was recorded on a CHI660D electrochemical analyser with a glassy carbon, Ag/AgCl and Pt wire electrode as the working, reference and auxiliary electrodes, respectively, using sodium borate buffer solutions (pH 9.0, 80 mM) as a supporting electrolyte at room temperature with a scanning rate of 100 mV s^{-1}. Dynamic light scattering (DLS) measurements were carried out using a Zatasizer Nano 3600 instrument (Malvern Instruments Ltd.). UV-vis absorption spectra were recorded on a TU-1810 spectrophotometer (Beijing Purkinje General Instrument Co., Ltd.) equipped with a photomultiplier tube detector. Infrared spectra (2–4 wt% sample in KBr pellets) were recorded using a

Bruker VERTEX 70v FT-IR spectrometer. Elemental analysis of the catalysts was performed on a TJA ICP-atomic emission spectrometer (IRIS Advantage ER/S). X-Ray photoelectron spectra (XPS) were measured by ESCALAB250xi with X-ray monochromatisation.

Photocatalytic water oxidation

Photocatalytic water oxidation was performed as follows: the desired concentration of complex **1** (0-5.0 μM) was prepared by dissolving the appropriate amount of catalyst in a borate buffer solution (80 mM, pH 9.0) containing $[Ru(bpy)_3]Cl_2$ (1.0 mM) and $Na_2S_2O_8$ (5.0 mM). The above solution was deaerated by purging with Ar gas for 10 min in a flask (28 mL) sealed with a rubber plug (the total volume of the reaction solution was 15 mL). The reaction was then started by irradiating the solution with a LED light source (light intensity 15.8 mW, beam diameter 2 cm) through a transmitting glass filter ($\lambda \geq 420$ nm) at room temperature. After each sampling time, 100 μL of Ar was injected into the flask and then the same volume of gas sample in the headspace of the flask was withdrawn by a SGE gas-tight syringe and analyzed by gas chromatography (GC). The O_2 in the sampled gas was separated by passing through a 2 m × 3 mm packed molecular sieve 5 Å column with an Ar carrier gas and quantified by a Thermal Conductivity Detector (TCD). The total amount of evolved O_2 was calculated based on the concentration of O_2 in the headspace gas. Contamination of the head-space with air was corrected by measuring the N_2 concentration present in the head-space. The solution pH was monitored after the reaction by a METTLER TOLEDO FEP20 pH meter.

For flash photolysis experiments, 50 μM $[Ru(bpy)_3]Cl_2$ were used to investigate the stability of complex 1 instead of 1.0 mM $[Ru(bpy)_3]Cl_2$, which is limited by the instrument.

Definition of half-wave potential ($E_{1/2}$)

$E_{1/2} = (Epa + Epc) / 2$

Epa : the oxidation potential of $Ru(bpy)_3^{2+/3+}$

Epc : the reduction potential of $Ru(bpy)_3^{2+/3+}$

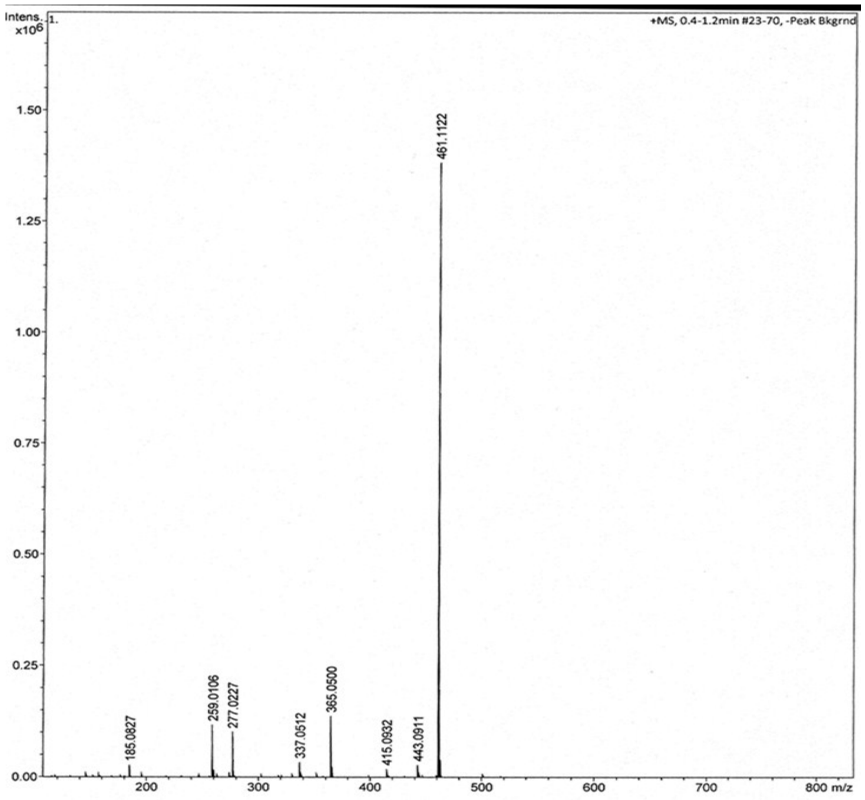

Fig. S1 ESI/MS of complex **1** in CH_3CN.

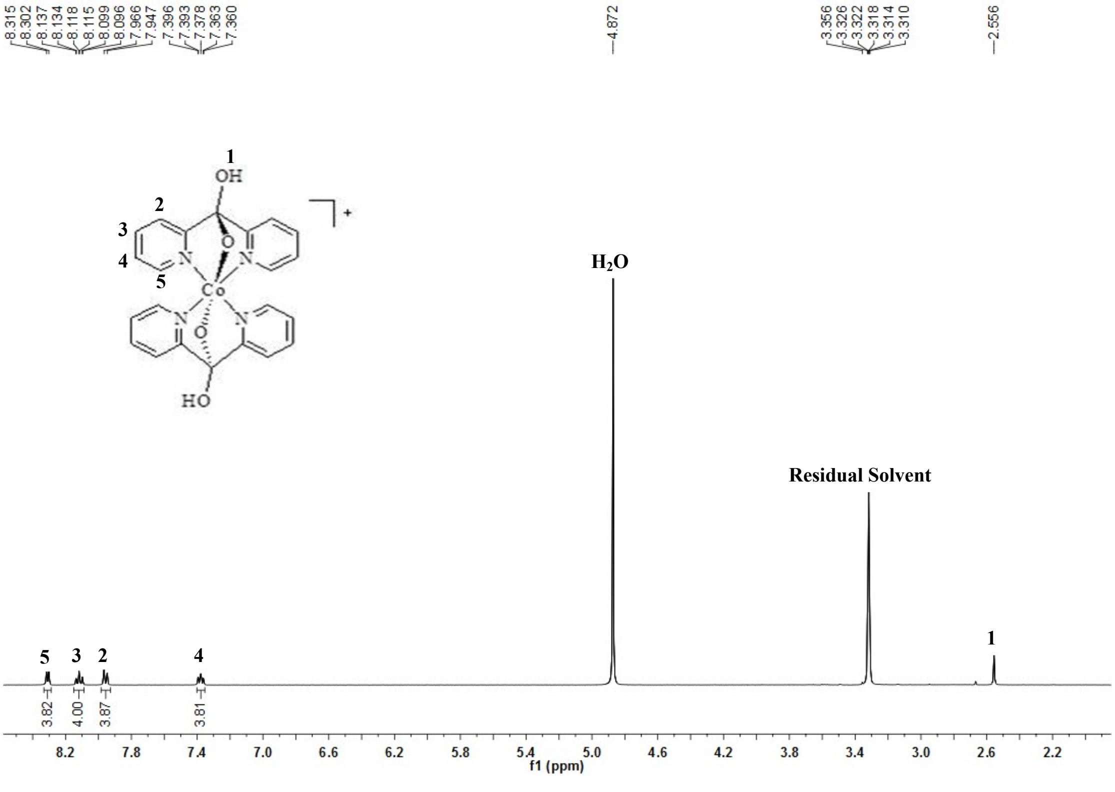

Fig. S2 ^1H NMR of **1** in CD_3OD. 1, 2.56ppm (s, 2H); 2, 7.95ppm (d, 4H); 3, 8.12ppm (m, 4H); 4, 7.38ppm (m, 4H); 5, 8.30ppm (d, 4H).

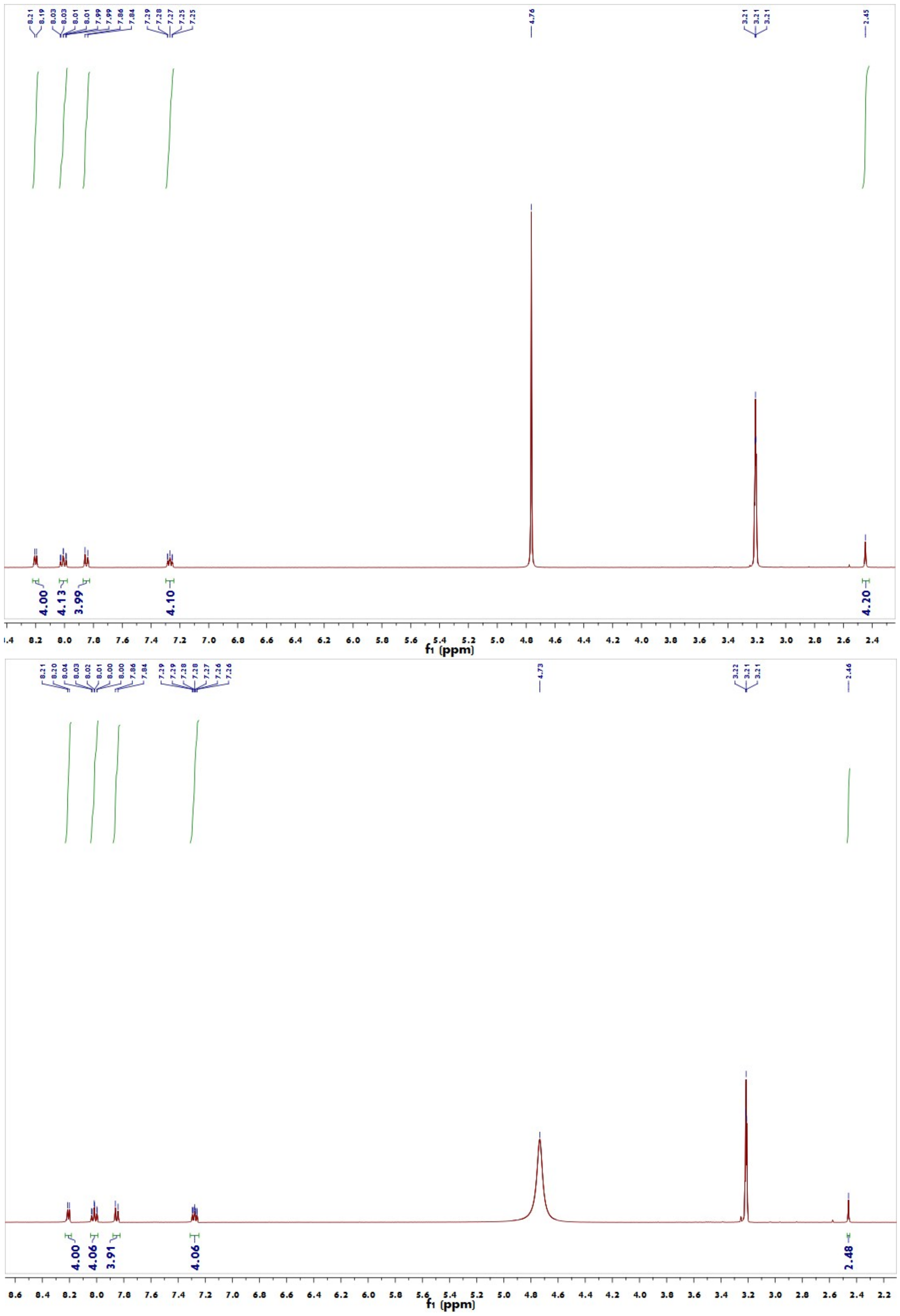

Fig. S3 ^{1}H NMR of **1** in CD_3OD (top); ^{1}H NMR of **1** in CD_3OD with two drops of D_2O (bottom).

After adding two drops of D_2O to solution, the peak integral area of ^{1}H in group OH obviously reduced to 2.48 from 4.20, which further certifies the attribution of the active hydrogen in Fig. S2. The active hydrogen is easy to exchange with D_2O.

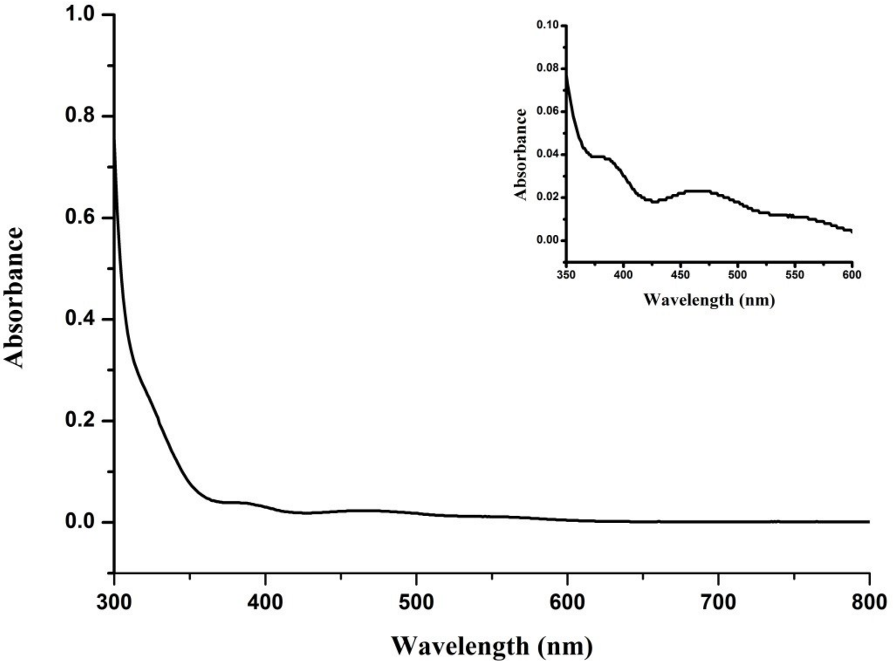

Fig. S4 UV-vis spectrum of 0.7 mM **1** in the sodium buffer (80mM, initial pH 9.0). Under the catalytic concentration, the absorbance peaks of complex **1** were hardly observed.

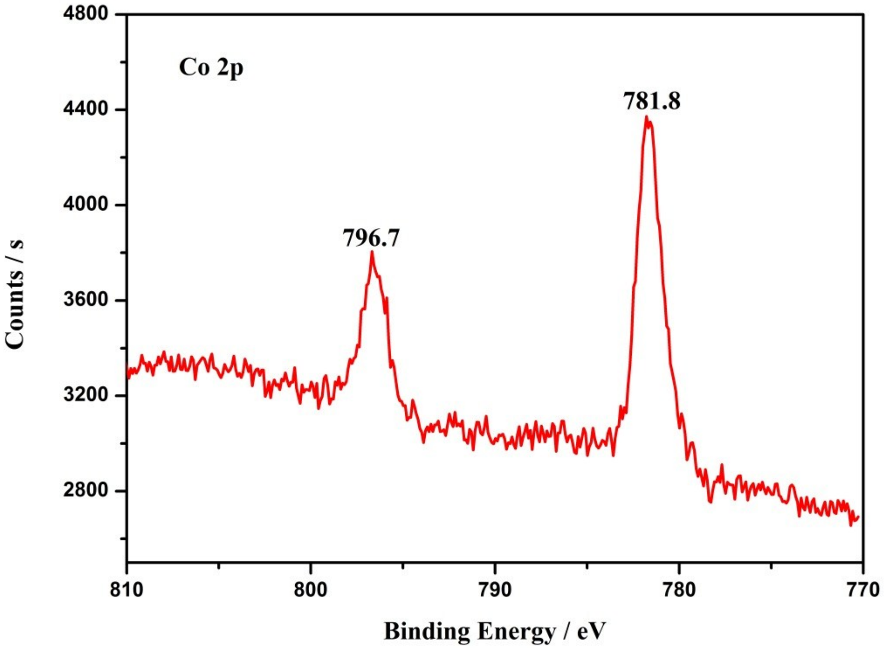

Fig. S5 X-Ray photoelectron spectrum of **1** showing the region of Co $2p_{3/2}$ and Co $2p_{1/2}$ peaks of **1**. The binding energy of each element was corrected by the C 1s peak (284.8 eV).

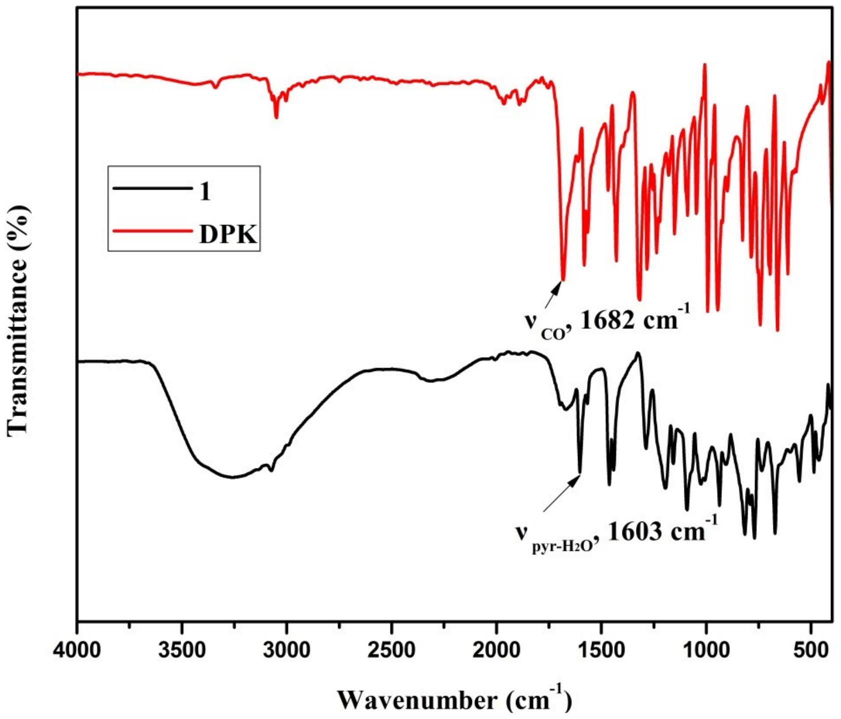

Fig. S6 The FT-IR spectra of complex **1** and DPK.

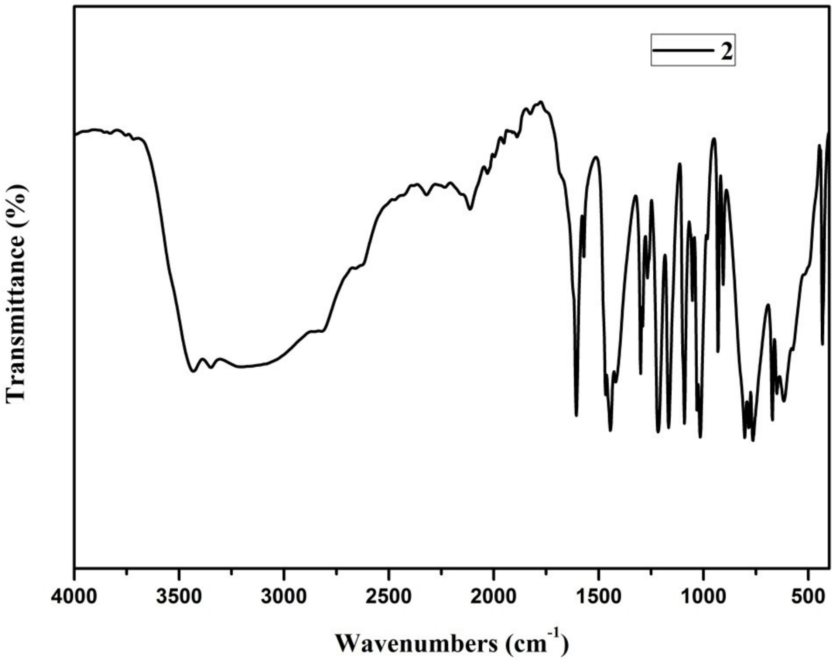

Fig. S7 The FT-IR spectrum of complex **2**.

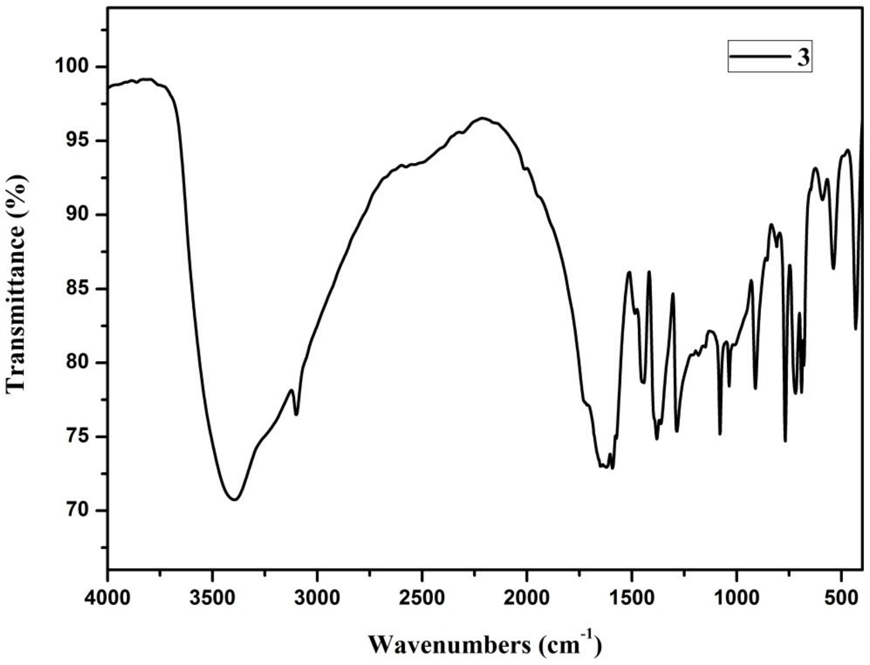

Fig. S8 The FT-IR spectrum of complex **3**.

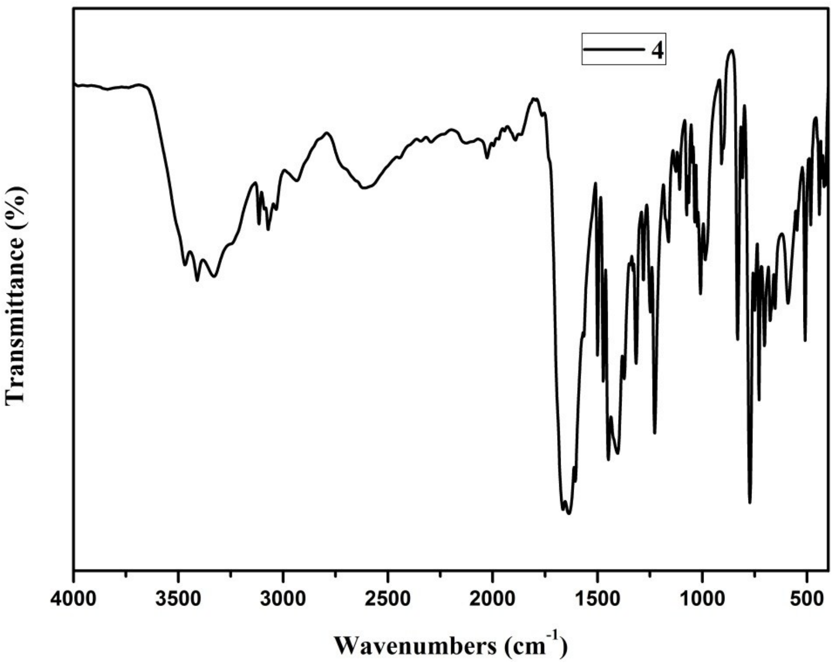

Fig. S9 The FT-IR spectrum of complex **4**.

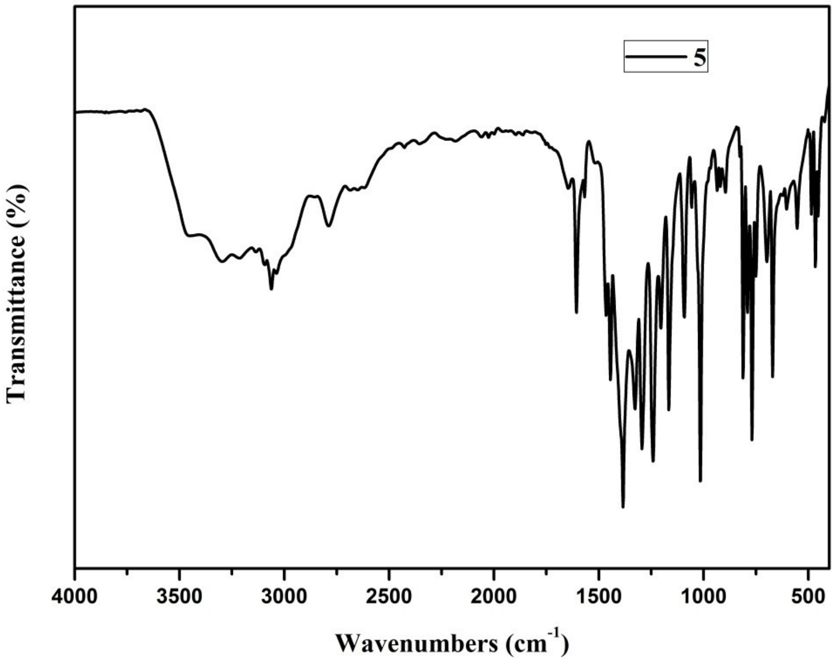

Fig. S10 The FT-IR spectrum of complex **5**.

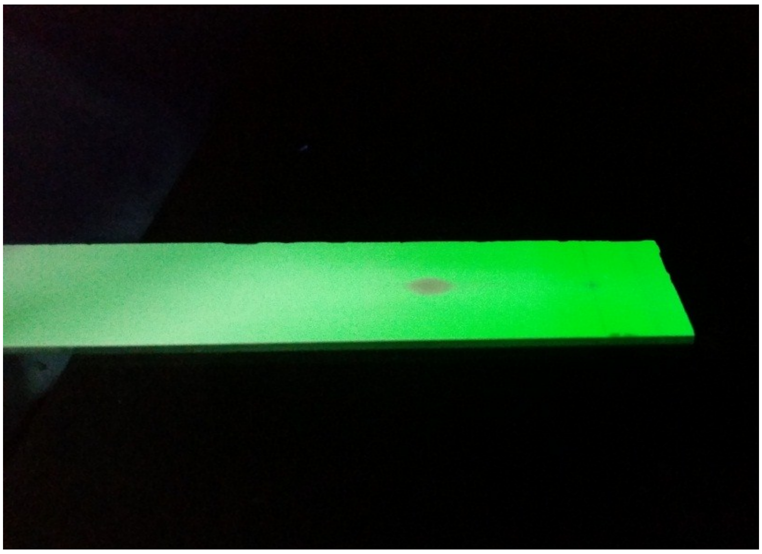

Fig. S11 Thin-layer chromatography (TLC) of **1**, using a methanol in dichloromethane mobile phase.

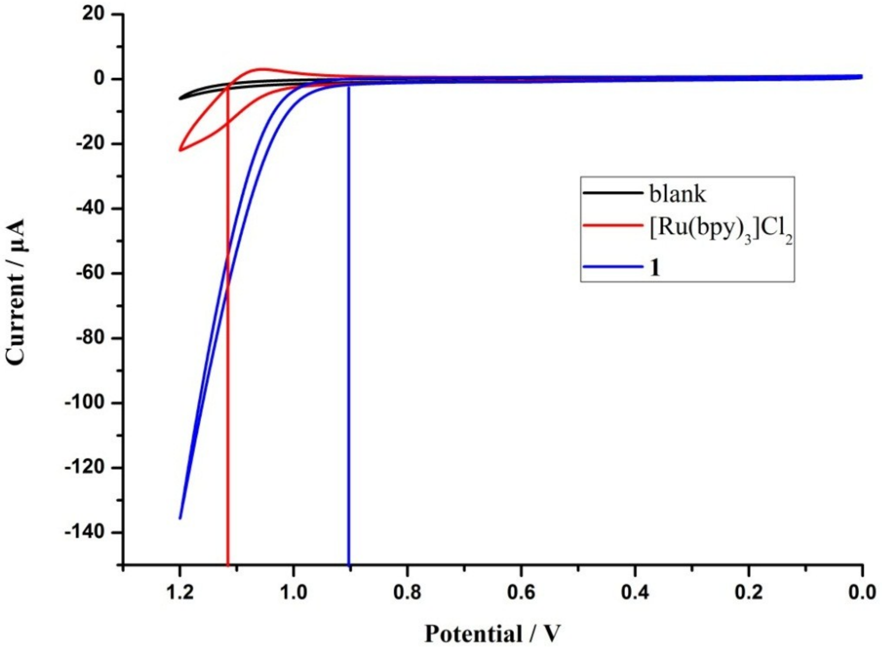

Fig. S12 Cyclic voltammograms (CVs) of 80 mM sodium borate buffer solution at pH 9.0 with 1.0 mM $[Ru(bpy)_3]Cl_2$ (red line) and 0.7 mM of **1** (blue line). The black line displays the CV of 80 mM sodium borate buffer solution (pH 9.0), Ag/AgCl electrode as reference.

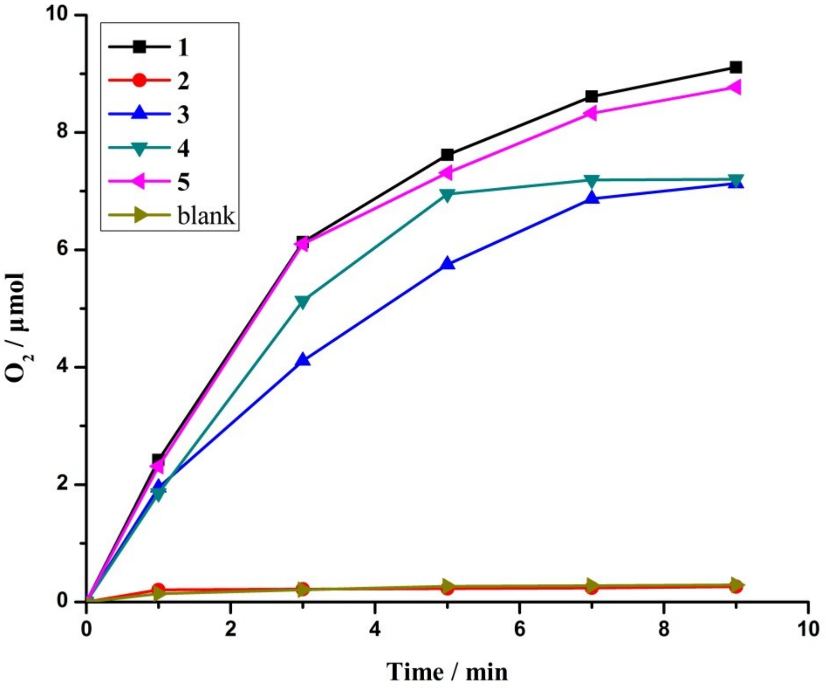

Fig. S13 Kinetics of O_2 formation in the photocatalytic system with different catalysts (**1**, black; **2**, red; **3**, blue; 5.0 μM **4**, dark cyan; **5**, magenta; blank, dark yellow).

Conditions: LED lamp (≥420 nm),15.8 mW; 5.0 μM catalyst, 1.0 mM $[Ru(bpy)_3]Cl_2$, 5.0 mM $Na_2S_2O_8$, 80 mM sodium borate buffer (pH 9.0); total reaction volume 15 mL and overall volume 28 mL; vigorous agitation using a magnetic stirrer.

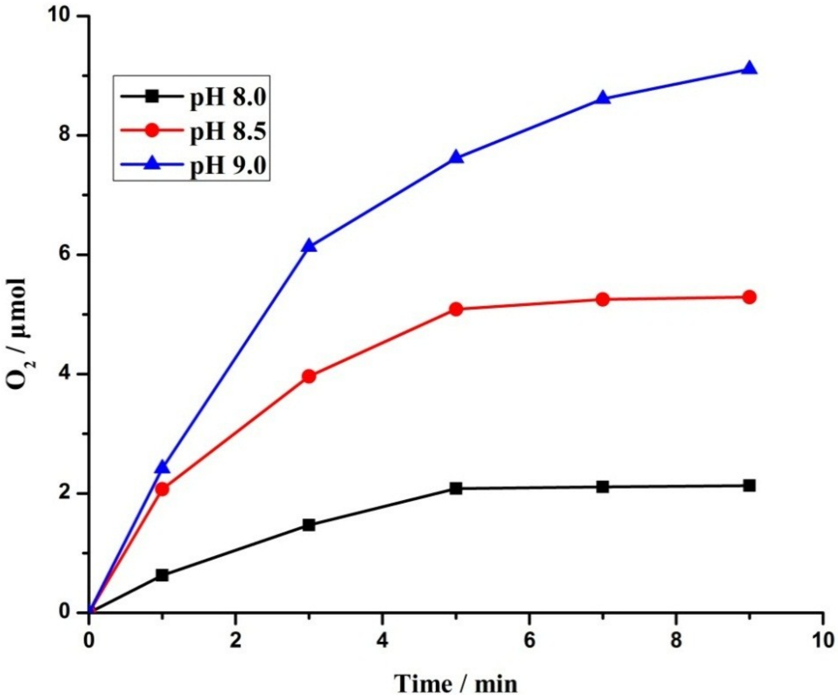

Fig. S14 Kinetics of O_2 formation in the photocatalytic system using 5.0 µM **1** with different pH (pH 8.0, black; pH 8.5, red; pH 9.0, blue).

Conditions: LED lamp (≥420 nm),15.8 mW; 1.0 mM $[Ru(bpy)_3]Cl_2$, 5.0 mM $Na_2S_2O_8$, 80 mM sodium borate buffer; total reaction volume 15 mL and overall volume 28 mL; vigorous agitation using a magnetic stirrer.

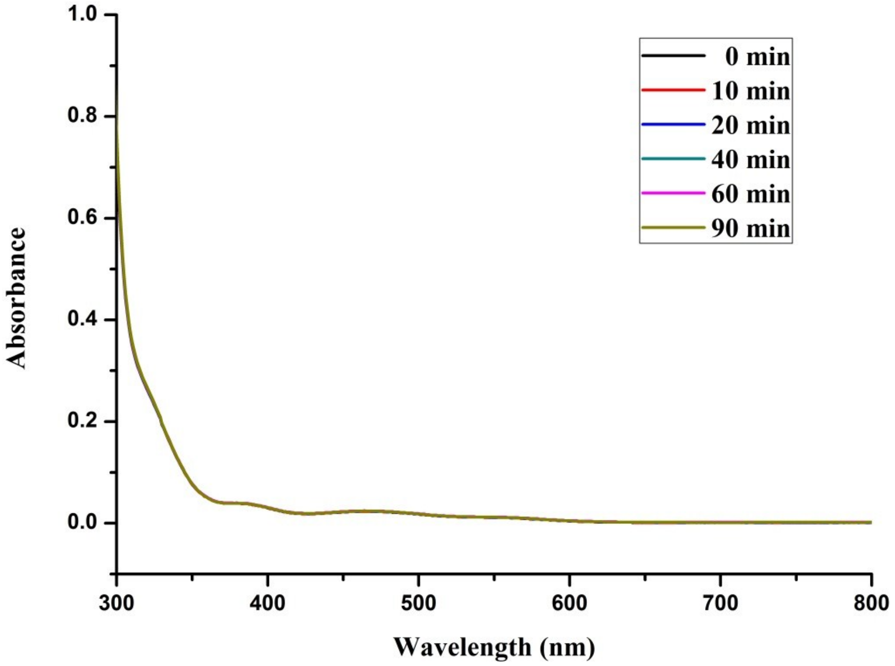

Fig. S15 Time-dependent UV-Vis spectra of **1** (0.7mM) in the sodium borate buffer solution (80 mM initial pH 9.0). The UV-Vis curves remained unchanged with time.

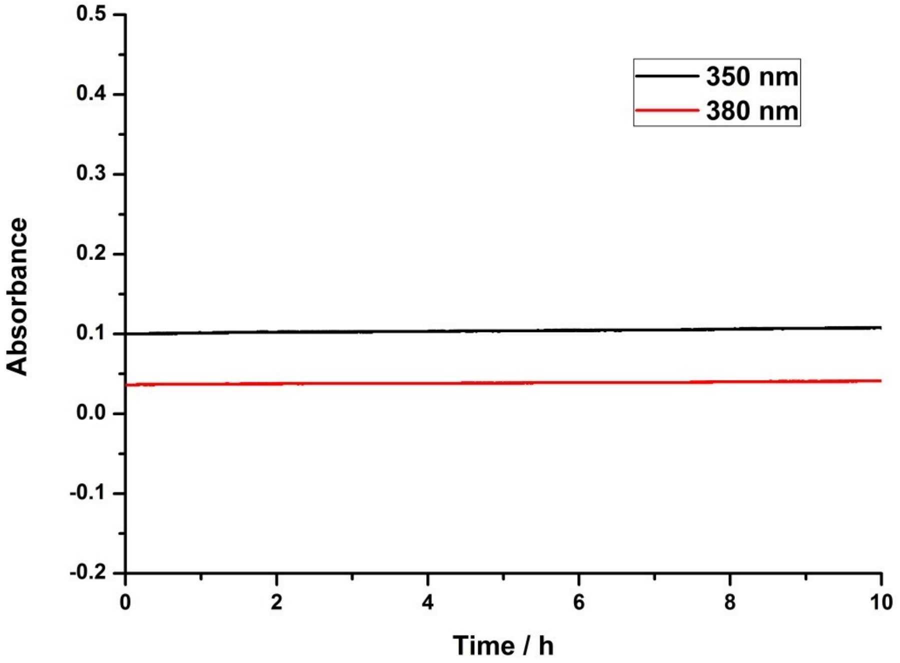

Fig. S16 Changes in UV-vis spectra of 0.7 mM **1** in the sodium borate buffer at pH 9.0 over a 10-hour period.

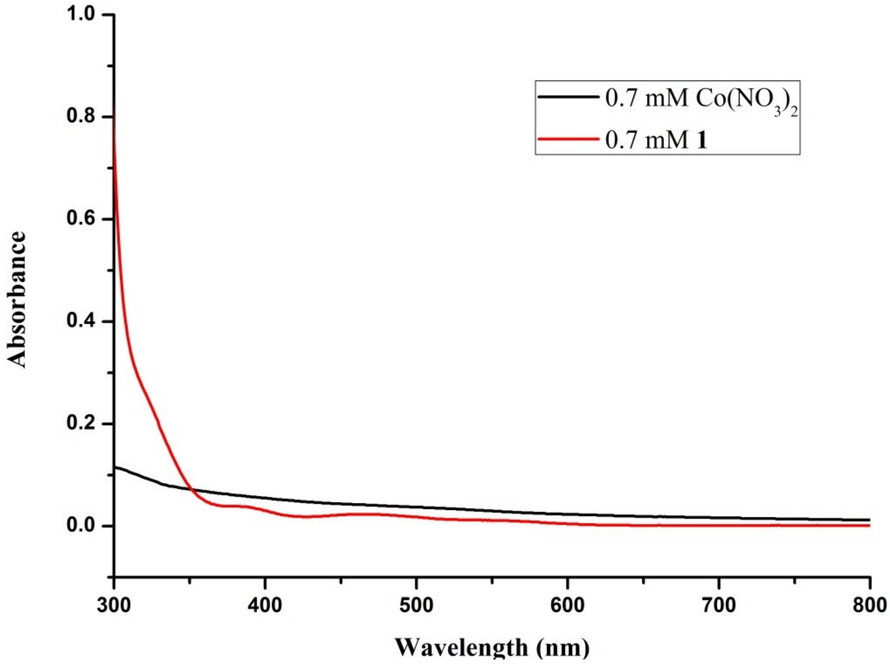

Fig. S17 UV-vis spectra of 0.7 mM $Co(NO_3)_2$ (black line) and 0.7 mM **1** (red line) in the sodium buffer (80mM, initial pH 9.0).

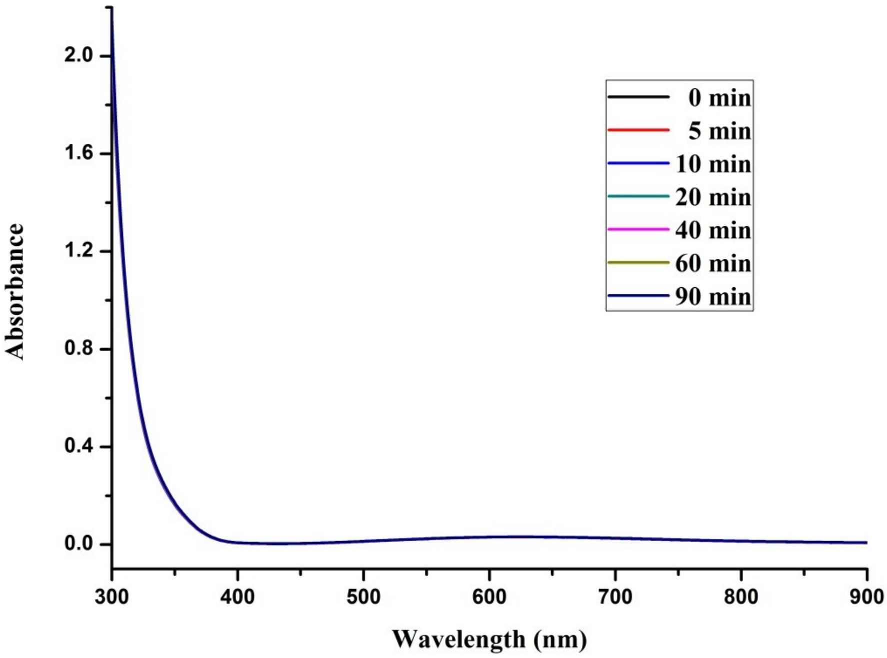

Fig. S18 Time-dependent UV-Vis spectra of **2** (0.7mM) in the sodium borate buffer solution (80 mM initial pH 9.0). The UV-Vis curves remained unchanged with time.

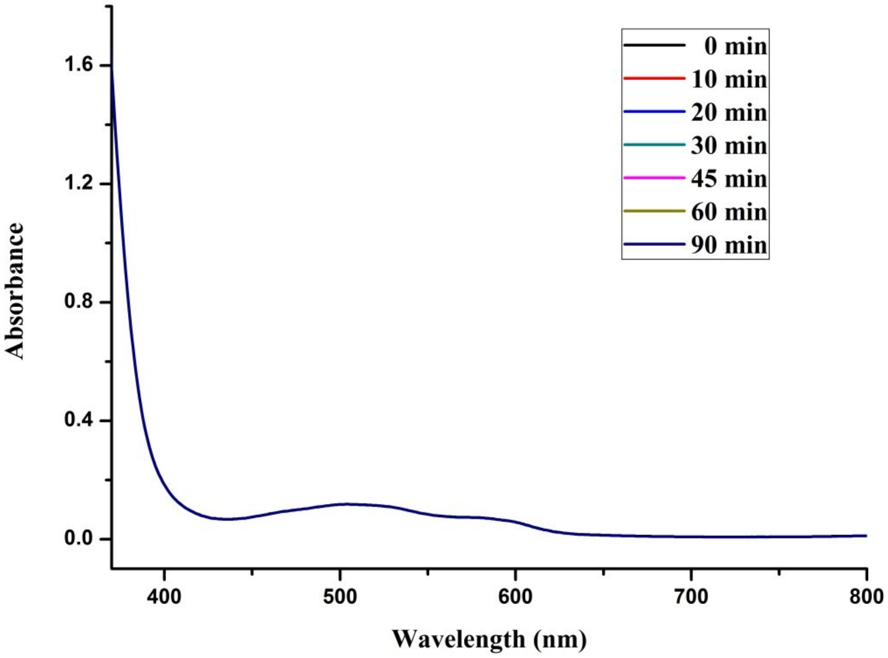

Fig. S19 Time-dependent UV-Vis spectra of **3** in the sodium borate buffer solution (80 mM initial pH 9.0). The UV-Vis curves remained unchanged with time.

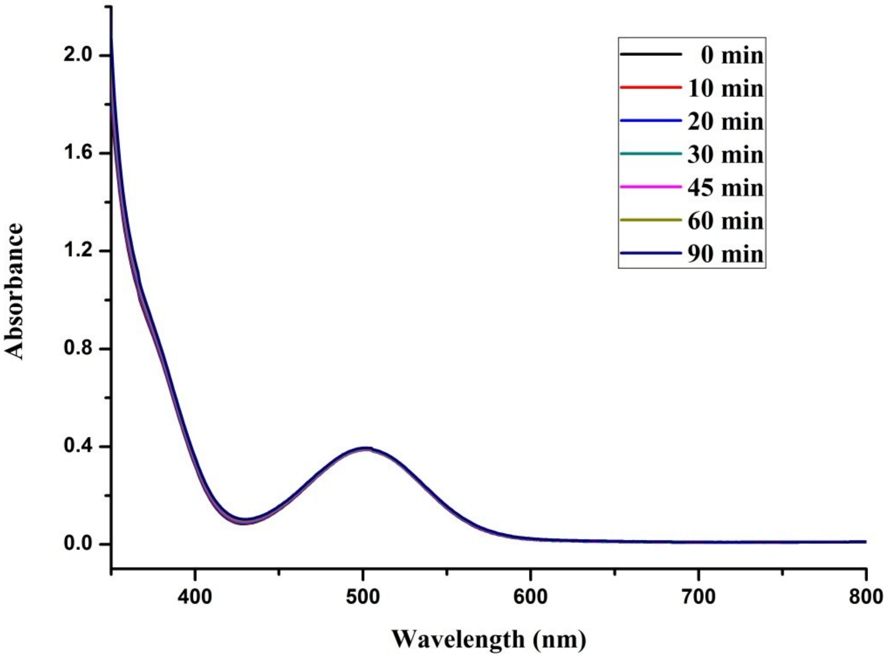

Fig. S20 Time-dependent UV-Vis spectra of **4** in the sodium borate buffer solution (80 mM initial pH 9.0). The UV-Vis curves remained unchanged with time.

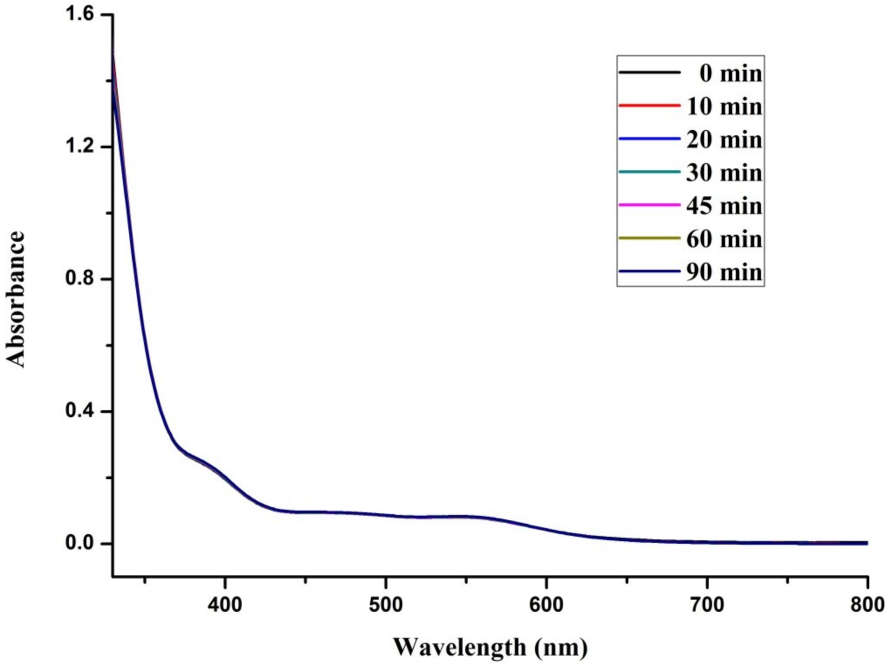

Fig. S21 Time-dependent UV-Vis spectra of **5** in the sodium borate buffer solution (80 mM initial pH 9.0). The UV-Vis curves remained unchanged with time.

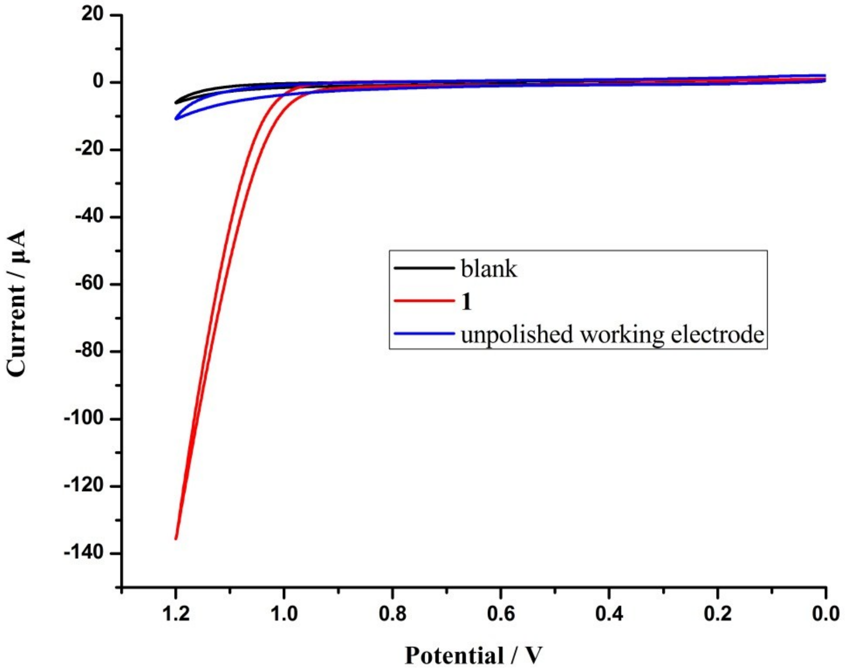

Fig. S22 Cyclic voltammograms (CVs) of 80 mM sodium borate buffer solution at pH 9.0 with 0.7 mM of **1** (red line) and unpolished working electrode after 10 min electro-deposition in borate buffer containing 0.7 mM complex **1** (blue line). The black line displays the CV of 80 mM sodium borate buffer solution (pH 9.0), Ag/AgCl electrode as reference. The blue curve demonstrates that no free cobalt ions exist in the reaction solution.

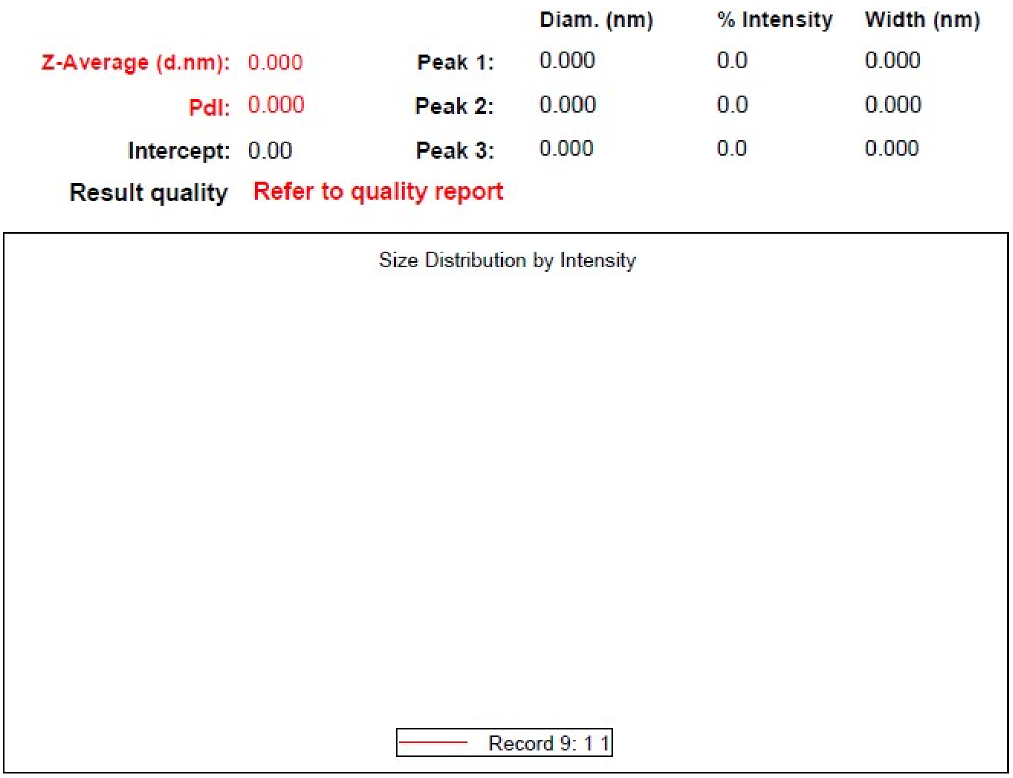
```
                                     Diam. (nm)   % Intensity   Width (nm)
Z-Average (d.nm):  0.000    Peak 1:  0.000        0.0           0.000
             PdI:  0.000    Peak 2:  0.000        0.0           0.000
       Intercept:  0.00     Peak 3:  0.000        0.0           0.000
  Result quality   Refer to quality report
```

Fig. S23 DLS measurement of a water oxidation reaction solution of **1** after 9 min of irradiation shows that no particles exist in photocatalytic water oxidation system. The detection limit of the instrument is 1-6000 nm.

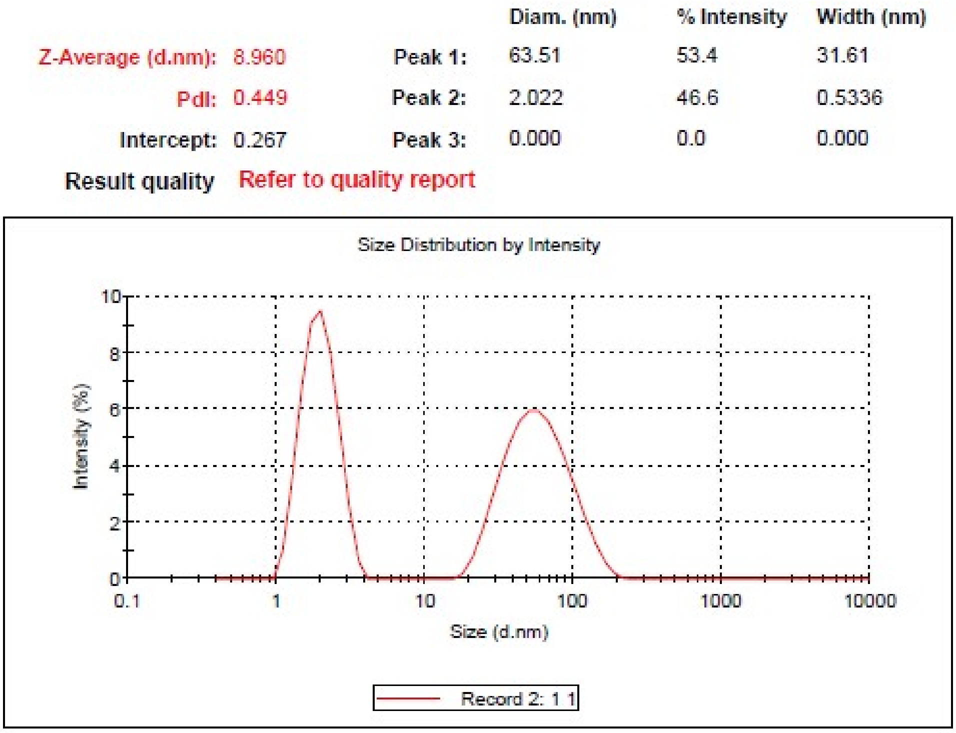

			Diam. (nm)	% Intensity	Width (nm)
Z-Average (d.nm):	8.960	Peak 1:	63.51	53.4	31.61
PdI:	0.449	Peak 2:	2.022	46.6	0.5336
Intercept:	0.267	Peak 3:	0.000	0.0	0.000

Result quality Refer to quality report

Fig. S24 DLS measurement of a water oxidation reaction solution of $Co(NO_3)_2$ after 9 min of irradiation shows that nanoparticles (2.02 and 63.51 nm) exist in photocatalytic water oxidation system.

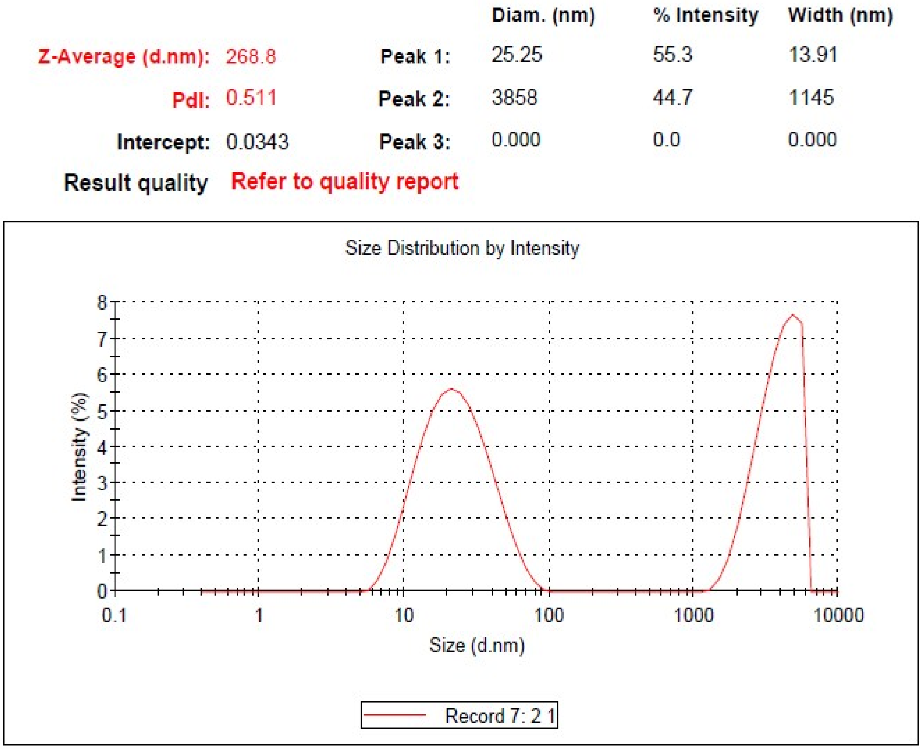

			Diam. (nm)	% Intensity	Width (nm)
Z-Average (d.nm):	268.8	Peak 1:	25.25	55.3	13.91
PdI:	0.511	Peak 2:	3858	44.7	1145
Intercept:	0.0343	Peak 3:	0.000	0.0	0.000

Result quality Refer to quality report

Fig. S25 DLS measurement of a water oxidation reaction solution of **3** after 9 min of irradiation shows that nanoparticles (25.25 nm) exist in photocatalytic water oxidation system.

			Diam. (nm)	% Intensity	Width (nm)
Z-Average (d.nm):	493.4	**Peak 1:**	4527	62.6	871.9
PdI:	0.833	**Peak 2:**	30.06	37.4	13.20
Intercept:	0.0470	**Peak 3:**	0.000	0.0	0.000

Result quality Refer to quality report

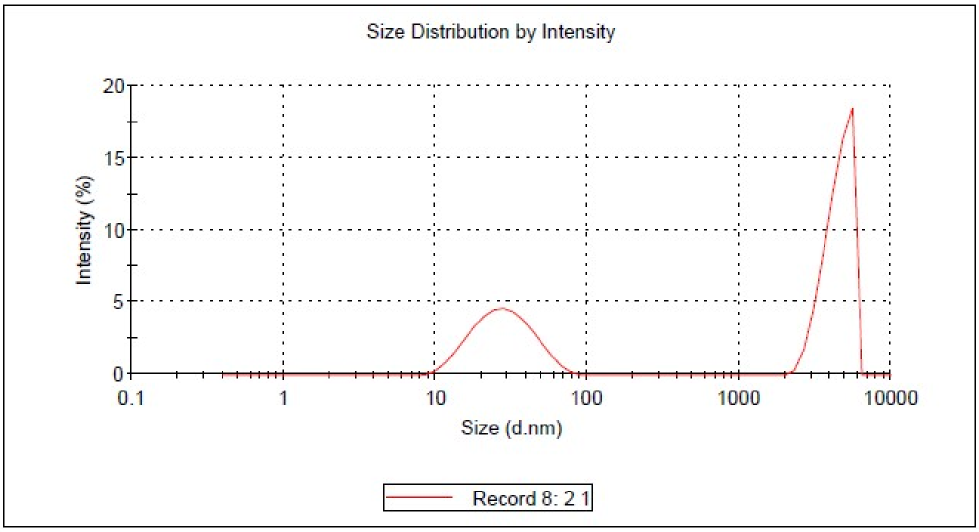

Fig. S26 DLS measurement of a water oxidation reaction solution of **4** after 9 min of irradiation shows that nanoparticles (30.06 nm) exist in photocatalytic water oxidation system.

			Diam. (nm)	% Intensity	Width (nm)
Z-Average (d.nm):	6.363e4	**Peak 1:**	0.8836	73.7	0.2398
PdI:	0.057	**Peak 2:**	5221	26.3	462.3
Intercept:	0.0581	**Peak 3:**	0.000	0.0	0.000

Result quality Refer to quality report

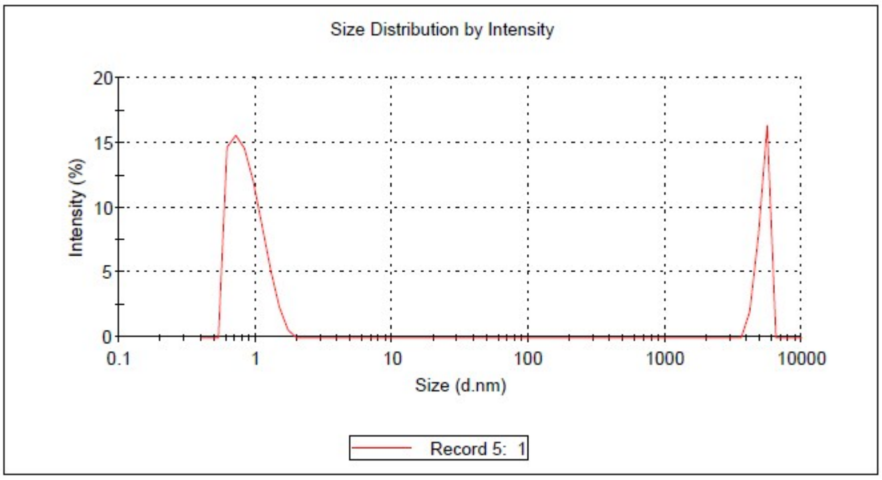

Fig. S27 DLS measurement of a water oxidation reaction solution of **5** after 9 min of irradiation shows that nanoparticles exist in photocatalytic water oxidation system.

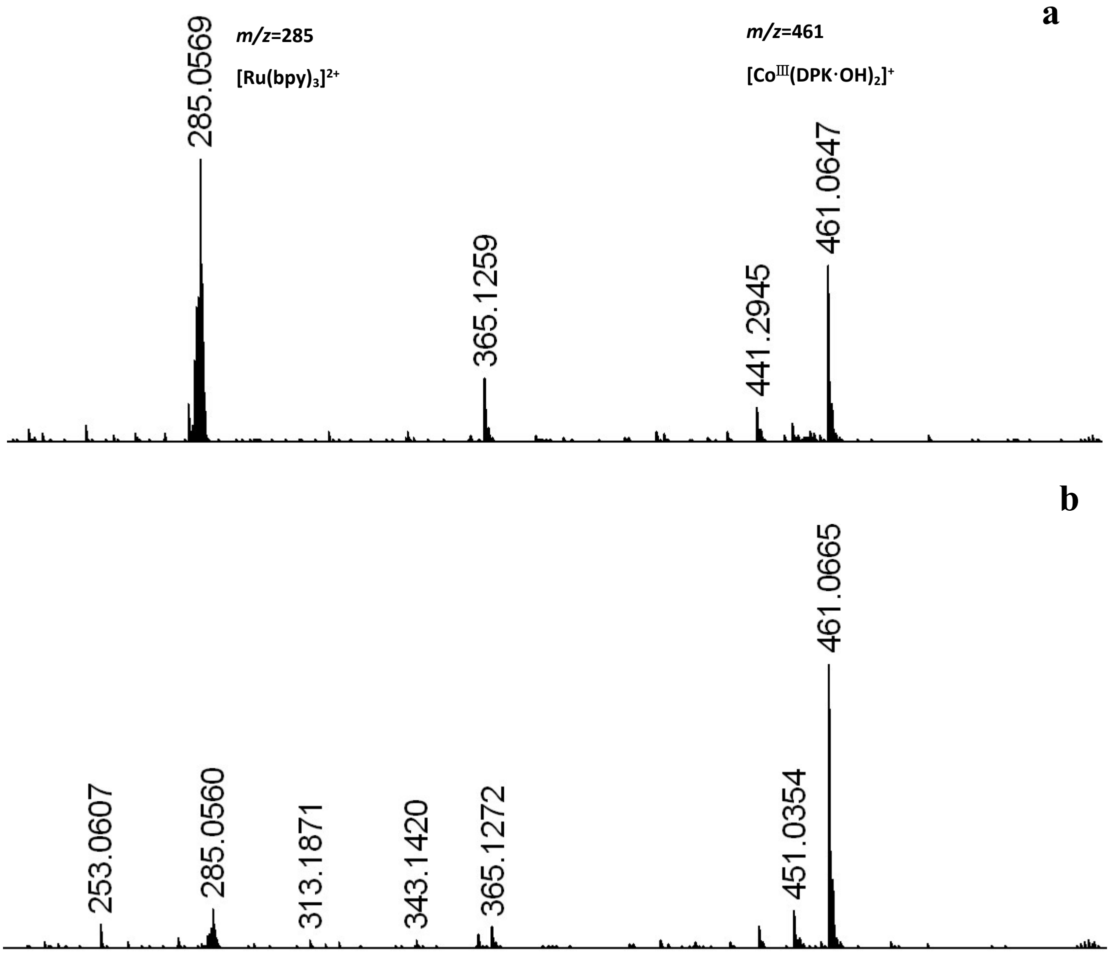

Fig. S28 HR-MS of a solution of **1** (0.1 mM) with [Ru(bpy)$_3$]Cl$_2$ (1.0 mM) and Na$_2$S$_2$O$_8$ (5.0 mM) at pH = 9.0 in borate buffer (20 mM) before (a) and after (b) irradiation with LED lamp. Due to qualitative analysis of complexes for HR-MS, two peaks are consistent with each other between (a) and (b). *m/z*=461 [Co^{III}(DPK·OH)$_2$]$^+$, *m/z*=285 [Ru(bpy)$_3$]$^{2+}$.

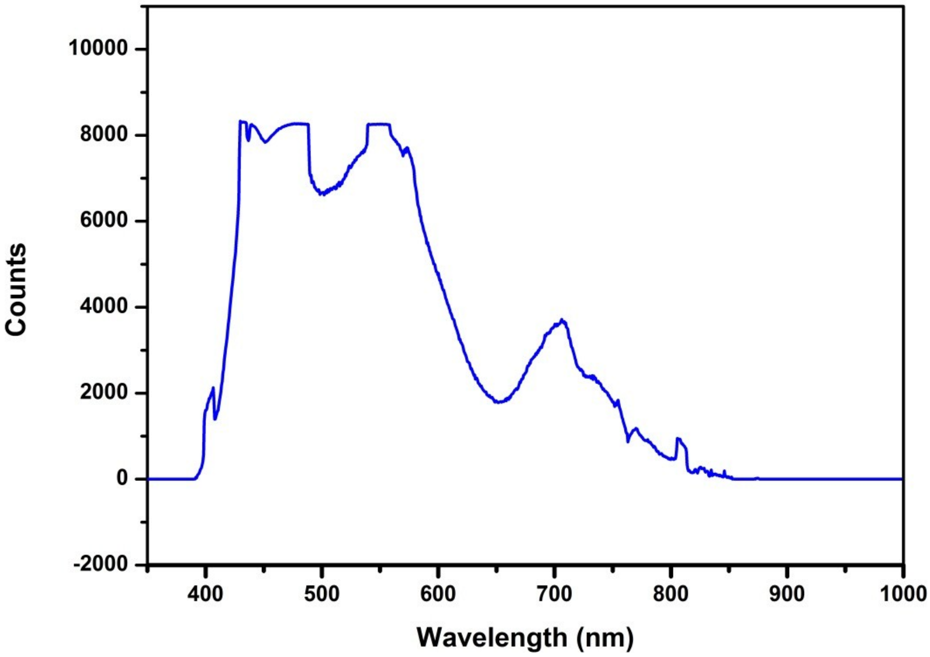

Fig. S29 The spectrum of LED lamp.

Table S1. Crystal and Refinement Data for Complexes **1**

complex	**1**
Identification code	$[Co(C_{11}H_9N_2O_2)_2]Cl$
Empirical formula	$C_{22}H_{18}CoN_4O_4Cl$
Formula weight	496.75
Temperature/K	288.5(5)
Crystal system	triclinic
Space group	P-1
a/Å	8.665(5)
b/Å	8.683(4)
c/Å	9.769(4)
α/°	80.53(4)
β/°	76.38(4)
γ/°	76.01(5)
Volume/$Å^3$	688.6(6)
Z	1
$\rho_{calc}g/cm^3$	1.112
μ/mm^{-1}	0.651
F(000)	237.0
Crystal size/mm^3	0.35 × 0.33 × 0.28
Radiation	MoKα (λ = 0.71073)
2Θ range for data collection/°	6.86 to 52.02
Index ranges	$-8 \leq h \leq 11$, $-7 \leq k \leq 11$, $-9 \leq l \leq 13$
Reflections collected	4080
Independent reflections	2441 [R_{int} =0.0774, R_{sigma} = 0.1930]
Data/restraints/parameters	2441/0/143
Goodness-of-fit on F^2	0.981
Final R indexes [I>=2σ (I)]	R_1 = 0.1031, wR_2 = 0.2855
Final R indexes [all data]	R_1 = 0.1601, wR_2 = 0.3166
Largest diff. peak/hole / e $Å^{-3}$	0.47/-0.47

Table S2. Photocatalytic water oxidation with different catalysts (5.0 μM).[a]

[Cat.]	TON[b]	O_2 yield (%)[c]	Hydrolytic Stability	Oxidative Stability
Complex **1**	122	24.3	YES	YES
Complex **2**	3.5	0.7	YES	_
Complex **3**	95	19.0	YES	NO
Complex **4**	96	19.2	YES	NO
Complex **5**	117	23.4	YES	NO

[a] Conditions: LED lamp (≥420 nm), 15.8 mW; 1.0 mM $Ru(bpy)_3Cl_2$, 5.0 mM $Na_2S_2O_8$, 5.0 μM **1-5**, 80 mM sodium borate buffer (initial pH 9.0); total reaction volume 15 mL and head space volume 13mL;

vigorous agitation using a magnetic stirrer. [b] TON = mole of O_2 / mole of catalyst. [c] O_2 Yield = 2 * mole of O_2 / mole of $Na_2S_2O_8$.

Table S3. TON and TOF of photocatalytic water oxidation catalyzed by different catalysts

Catalyst	Representative reaction conditions	TON	TOF	Ref.
1	LED lamp ($\lambda \geq 420$ nm), 0.2 μM catalyst, 1.0 mM $[Ru(bpy)_3]Cl_2$, 5.0 mM $Na_2S_2O_8$, 80 mM sodium borate buffer (pH 9.0)	1610	11.1 s^{-1}	This work
2	LED lamp ($\lambda \geq 420$ nm), 5.0 μM catalyst, 1.0 mM $[Ru(bpy)_3]Cl_2$, 5.0 mM $Na_2S_2O_8$, 80 mM sodium borate buffer (pH 9.0)	3.5	0.05 s^{-1}	This work
3		95	0.43 s^{-1}	This work
4		96	0.41 s^{-1}	This work
5		117	0.51 s^{-1}	This work
CoFPS	300 W Xe lamp, 1.0 μM catalyst, $[Ru(bpy)_3](NO_3)_2$ (0.2 mm), $Na_2S_2O_8$ (7.0 mm) and 100 mM borate buffer (pH 9.0) under Ar at 20 °C.	570	1.1s^{-1}	4
$[(TPA)Co(\mu\text{-}OH)(\mu\text{-}O_2)Co(TPA)](ClO_4)_3$	LED lamp (460-480nm), 5.0 μM catalyst, $[Ru(bpy)_3](ClO_4)_2$ (0.4 mm),and $Na_2S_2O_8$ (3 mm) in borate buffer (50 mm, pH 8).	63	2.0 s^{-1}	5
$[Co^{II}(Me_6tren)(OH_2)]^{2+}$	Xe lamp (λ> 420 nm) , 50 mM phosphate buffer solution (pH 8.0) containing $[Ru(bpy)_3]^{2+}$ (0.50 mM), $Na_2S_2O_8$ (10 mM) and catalyst (50 mM)	54	No data	6
$[Co^{III}(Cp^*)(bpy)(OH_2)]^{2+}$		29	No data	
Salen Co(II)	LED lamp ($\lambda \geq 420$ nm), 1.6 μM catalyst, 1.0 mM $[Ru(bpy)_3](ClO_4)_2$, 5.0 mM $Na_2S_2O_8$, 80 mM sodium borate buffer (pH 9.0)	854	6.4 s^{-1}	7
CoTCPP		191	No data	
CoSlp		531	No data	
Trans-$[Co^{II}(qpy)(OH_2)_2](ClO_4)_2$	500 W mercury arc lamp (457 nm), 0.2 μM catalyst, 128 μM $[Ru(bpy)_3]Cl_2$, 5 mM $Na_2S_2O_8$, 15 mM borate buffer solution (pH 8.0).	355	No data	8
$Co^{III}{}_4O_4(OAc)_4$	250 W high power Arc lamp (450 nm), 41.5 μM catalyst, 0.5 mM	40	0.02 s^{-1}	9

$(py)_4$	$[Ru(bpy)_3]Cl_2$, 10.5 mM $Na_2S_2O_8$, HCO_3- buffer (pH 7.0).,			
$[Co^{II}_4(hmp)_4(\mu\text{-}OAc)_2(\mu_2\text{-}OAc)_2(H_2O)_2]$	LED lamp (470nm), 60 μM catalyst , 1 mM $[Ru(bpy)_3]^{2+}$, 5 mM $Na_2S_2O_8$,borate buffer (pH 9.0)	28	7.0 s^{-1}	10
$Ru^{II}(hqc)(pic)_3$	A xenon lamp (500 W) with a $\lambda > 400$ nm filter, 10 mL of pH 7.2 phosphate buffer (20 mM), 0.55 mL of acetonitrile, 55.0 μM catalyst, 550 μM $[Ru(bpy)(dcbpy)_2]^{2+}$, and $[S_2O_8^{2-}] = 10$ mM.	61	No data	11
$[Fe(cyclen)Cl_2]Cl$	[Catalyst] = 1.0 mM, $[Ru(bpy)_3Cl_2]$ = 0.2 mM, $[Na_2S_2O_8]$ = 2 mM in 15 mM borate buffer (pH 8.5) at 23 °C, $\lambda > 420$ nm.	412	No data	12
$[NiL_3](ClO_4)_2$	$[Ru(bpy)_3](ClO_4)_2$ (0.12 mM), catalyst (0.6 μM), and $Na_2S_2O_8$ (2.5 mM) in 30 mM borate buffer (pH 8.0), T = 23 °C 500 W Xe lamp (λ = 457 nm).	855	No data	13

1. V. A. Kawade, A. S. Kumbhar, D. B. Naik and R. J. Butcher, *Dalton Trans*, 2010, **39**, 5664-5675.
2. J. Qi, X. S. Zhai, H. L. Zhu and J. L. Lin, *Acta Cryst.*, 2014, **C70**, 198-201.
3. B. F. Abrahams, T. A. Hudson and R. Robson, *Chem. Eur. J.*, 2006, **12**, 7095-7102.
4. T. Nakazono, A. R. Parent and K. Sakai, *Chem. Eur. J.*, 2015, **21**, 6723-6726.
5. H. Y. Wang, E. Mijangos, S. Ott and A. Thapper, *Angew. Chem. Int. Ed.*, 2014, **53**, 14499-14502.
6. D. Hong, J. Jung, J. Park, Y. Yamada, T. Suenobu, Y.-M. Lee, W. Nam and S. Fukuzumi, *Energy Environ. Sci.*, 2012, **5**, 7606-7616.
7. S. Fu, Y. Liu, Y. Ding, X. Du, F. Song, R. Xiang and B. Ma, *Chem. Commun.*, 2014, **50**, 2167-2169.
8. C.-F. Leung, S.-M. Ng, C.-C. Ko, W.-L. Man, J. Wu, L. Chen and T.-C. Lau, *Energy Environ. Sci.*, 2012, **5**, 7903-7907.
9. N. S. McCool, D. M. Robinson, J. E. Sheats and G. C. Dismukes, *J. Am. Chem. Soc.*, 2011, **133**, 11446-11449.
10. F. Evangelisti, R. Guttinger, R. More, S. Luber and G. R. Patzke, *J. Am. Chem. Soc.*, 2013, **135**, 18734-18737.
11. L. Tong, Y. Wang, L. Duan, Y. Xu, X. Cheng, A. Fischer, M. S. Ahlquist and L. Sun, *Inorg. Chem.*, 2012, **51**, 3388-3398.
12. G. Chen, L. Chen, S.-M. Ng, W.-L. Man and T.-C. Lau, *Angew. Chem. Int. Ed.*, 2013, **52**, 1789 - 1791.
13. G. Chen, L. Chen, S. M. Ng and T. C. Lau, *ChemSusChem*, 2014, **7**, 127-134.